

ACKNOWLEDGEMENT

Alhamdulillah, praise be to Almighty Allah S.W.T., the Most Gracious and the Most Merciful. First and foremost, I would like to express my appreciation and wholehearted sense of gratitude to my supervisor Dr Mohamad Aizat Abas for his continually guidance and constant support. His great interest and assistance has significantly contributed in bringing the success of this research study. Thank you for his invaluable efforts and continuous encouragement in correcting mistakes and also suggesting improvements. My sincere thanks to my co-supervisor, Prof. Ir. Dr. Mohd. Zulkifly Abdullah who has given me a very helpful advice and comments throughout this project.

I would like to express my appreciation to technical staffs of School of Mechanical Engineering, and Jabil Circuit Sdn Bhd especially Mr. Fakhrozi Che Ani for the excellent facilities and warm welcome. I also wish to extend my appreciation to Mr. M.Y. Tura and Mr. A. Marzukhi (Jabil Circuit Sdn Bhd) for their technical support and also MyBrain scholarship under the Malaysian Ministry of Education.

I would like to acknowledge this research work was partly supported by FRGS grant, FRGS/1/2015/TK03/USM/03/2, Short Term Grant, 60313020 from the Division of Research and Innovation, Universiti Sains Malaysia and Universiti Kebangsaan Malaysia (Research grant–DIP-2014-012).

Last but not least, I would like to convey my deepest appreciation to my beloved family, all friends and colleagues, for their endless love, prayer and encouragement.

	Page
ACKNOWLEDGEMENT	ii
TABLE OF CONTENTS	iii

TABLE OF CONTENTS

LIST OF TABLES	vii
LIST OF FIGURES	viii
LIST OF ABBREVIATIONS	xiii
LIST OF SYMBOLS	xvi
ABSTRAK	xix
ABSTRACT	xxi
 CHAPTER ONE: INTRODUCTION	
1.1 Introduction	1
1.2 Surface mount devices and technologies	2
1.2.1 Soldering process and materials	5
1.3 Problem statement	7
1.4 Objectives	8
1.5 Scopes and limitation	9
1.6 Thesis outline	10
 CHAPTER TWO: LITERATURE REVIEW	
2.1 Introduction	11

2.2	Electronic packaging and surface mount technologies	12
2.3	Miniaturization of surface mount component: 01005 capacitor	13
2.4	Nano-reinforced lead (Pb) free solder	18
2.5	Wettability and intermetallic compound	25
2.6	Numerical and experimental approach	28
2.7	Summary	32

CHAPTER THREE: RESEARCH METHODOLOGY

3.1	Introduction	34
3.2	Experimental setup in reflow process	36
3.2.1	Surface mount device: Ultra-fine package assembly	36
3.2.2	Reflow process: Temperature profile	38
3.2.3	Nano-reinforced lead free solder	41
3.3	Model development-FLUENT	43
3.3.1	Modelling equations	45
3.3.1(a)	Volume of fluid (VOF)	46
3.3.1(b)	Disperse phase model (DPM)	51
3.3.1(c)	Non-spherical formulation	56

3.3.1(d)	Fillet height calculation	58
3.3.2	Modelling and mesh development	59
3.3.3	Boundary condition	61
3.4	Grid independent test	63
3.5	FVM-DPM setup for the simulation model	67
3.6	Summary	68

CHAPTER FOUR: RESULTS AND DISCUSSIONS

4.1	Introduction	69
4.2	Experimental validation	70
4.2.1	Reflow process: Temperature profile	76
4.2.2	Intermetallic compound (IMC) layer and wetting formation	78
4.3	Numerical simulation	82
4.3.1	Nanoparticles distribution	83
4.3.2	Wetting formation	88
4.3.2 (a)	Wetting time	89
4.4	Wettability and fillet height	91
4.5	Velocity distribution	96

4.6	Pressure distribution and micro-voids	99
4.7	Optimization	101
4.8	Summary	103

CHAPTER FIVE: CONCLUSIONS

5.1	Statement of conclusion	104
5.2	Recommendations of future work	107

REFERENCES	109
-------------------	-----

APPENDICES

APPENDIX A

APPENDIX B

LIST OF PUBLICATIOND AND PRESENTATIONS

LIST OF TABLES

	Page
Table 3.1: Temperature setting in heating zones	41

Table 3.2:	Properties of 96.5Sn-3.0Ag-0.5Cu solder paste	42
Table 3.3:	Properties of titanium dioxide (TiO ₂), nickel oxide (NiO) and Iron (III) oxide (Fe ₂ O ₃)	42
Table 3.4:	Dimensions of the model components, reflow oven environment, FR4-PCB and ultra-fine 01005 capacitor in Ansys geometry and meshing model	61
Table 3.5:	Grid independent study by depicting the grid resolutions of 0.01 wt.% NiO	66
Table 4.1:	The trajectory of the different types of nanoparticles at different weight percentages (20µm scale).	72
Table 4.2:	Comparison between temperature profiles at the wetting zone	76
Table 4.3:	Flow Front pattern for the traceability of the TiO ₂ nanoparticles	85
Table 4.4:	Flow Front pattern for the traceability of the NiO nanoparticles	86
Table 4.5:	Flow Front pattern for the traceability of the Fe ₂ O ₃ nanoparticles	87
Table 4.6:	2D model-view of wetted SAC305 with trajectory of nanoparticles	93
Table 4.7:	Percentage differences of the simulation studies to the experimental results	95

LIST OF FIGURES

	Page
Figure 1.1: Printed Circuit Board (PCB)	2
Figure 1.2: PCB assembly method (a) SMT and (b) THT (Lee, 2002)	3
Figure 1.3: The evolution of the miniature sizes of passive component (Shah et al., 2006)	4
Figure 1.4: Schematic of SMT reflow oven (Tavarez and Gonzalez, 2003)	5
Figure 1.5: Schematic diagram of Sn-Ag-Cu eutectic structure	6
Figure 2.1: Active and passive components of SMT mounted on PCB	13
Figure 2.2: Configurations of passives component (a) disperse (b) integrated and (c) embedded (Lee et al., 2005)	14
Figure 2.3: The size distribution for passive component (Lasky, 1998)	15
Figure 2.4: EIA standard for SMD component (Grade, 2011)	15
Figure 2.5: External body of MLCC capacitor (Engel et al., 2006)	16
Figure 2.6: Internal body of MLCC capacitor (Engel et al., 2006)	17
Figure 2.7: Comparison MLCC capacitor to others capacitor available	18
Figure 2.8: List of recommended lead-free solder internationally (Ho et al., 2007)	20
Figure 2.9: Nanoparticles as the reinforcement material to the lead free solder (Chellvarajoo and Abdullah, 2016)	21
Figure 2.10: The morphology of (a) SAC305 and (b) Fe ₂ NiO ₄ nanoparticles (Chellvarajoo et al., 2015)	23
Figure 2.11: Mechanical properties presented in bar graph (a) micro hardness and (b) tensile strength of the nanocomposite solder (Chang et al., 2011)	24

Figure 2.12:	Intermetallic compound (IMC) layer (Nishikawa and Iwata, 2015)	26
Figure 2.13:	Interaction for the formation of IMC between Cu_6Sn_5 and Ag_3Sn nanoparticles (Rossi et al., 2016)	27
Figure 2.14:	Growth of IMC layer for different types of lead free solder (Tay et al., 2013)	27
Figure 2.15:	The particles tracked moves in the fluid (Kharoua et al., 2015)	30
Figure 2.16:	The trajectory of the particles and size distribution (Kharoua et al., 2015)	31
Figure 3.1:	Flowchart of methodology	35
Figure 3.2:	The size of the capacitor as the technology growth	37
Figure 3.3:	Internal structure of 01005 capacitor	38
Figure 3.4:	Typical convection SMT reflow oven	39
Figure 3.5:	FR4-PCB with mounted 01005 capacitor (ultra-fine package)	39
Figure 3.6:	Reflow thermal profile of nano-reinforced lead-free solder (Tsai, 2009)	40
Figure 3.7:	Flowchart of numerical setup in Ansys-Fluent	44
Figure 3.8:	Outline of 01005 capacitor model	45
Figure 3.9:	Surface tension of the molten solder between the solid and the fluid (liquid – molten solder) domain (Abtew and Selvaduray, 2000)	48
Figure 3.10:	Interaction of the particle with the thermophoretic force	53
Figure 3.11:	Brownian motion of nano-reinforced lead free solder	54

Figure 3.12:	The measurement illustration of the fillet height for the 01005 capacitor	58
Figure 3.13:	Meshing grid of (a) reflow oven environment and (b) FR4-PCB with mounted 01005 capacitor (ultra-fine package)	60
Figure 3.14:	Magnification of the 3D mesh model for ultra-fine 01005 capacitor on an FR4-PCB	61
Figure 3.15:	Schematic diagram of initial condition and boundary condition	62
Figure 3.16:	Meshing grid (a) 01005 capacitor mounted on PCB and (b) 01005 capacitor	64
Figure 3.17:	Computational meshing of the model, medium meshing (a) and (b), and fine meshing (c) and (d)	65
Figure 3.18:	Figure 3.18: CFD result in regular meshes and correlation expectation (Oliveira et al., 2017).	66
Figure 3.19:	Mesh independent analysis graph	67
Figure 4.1:	(a) 01005 capacitor with nano-reinforced lead free solder before the soldering process and (b) after the soldering process	70
Figure 4.2:	Fillet requirement for the 01005 capacitor (a) 3D view of the component (b) side view of the component (IPC, 2010)	71
Figure 4.3:	The lamella preparation of the ultra-fine solder joint	71
Figure 4.4:	EDS pattern for traceability Titanium (Ti) elements in solder joint	74
Figure 4.5:	EDS pattern for traceability Nickle (Ni) elements in solder joint	74

Figure 4.6:	EDS pattern for traceability Iron (Fe) elements in solder joint	75
Figure 4.7:	Temperature profile for nanocomposite solder	77
Figure 4.8:	The wetting formation at wetting zone of the temperature profile	78
Figure 4.9:	Composite solder wetting mechanism (a) composite solder on PCB pad (b) molten solder spreading and wetted, (c) diffusion of the molten solder and (d) formation of the intermetallic compound layer	79
Figure 4.10:	Schematic diagram of the IMC reaction stages under reflow soldering process of SMT	81
Figure 4.11:	HRTEM view of 01005 capacitor with nanocomposite solder (a) tilt view and (b) side view	82
Figure 4.12:	Logarithm plot of viscosity against particle volume concentration (J.Jeong at al., 2013).	84
Figure 4.13:	3D model-view of wetted SAC305 with nanoparticles	89
Figure 4.14:	Plot of wetting time for different types and weight percentages of nanoparticles	85
Figure 4.15:	The measurement illustration of the fillet height for the 01005 capacitor (ultra-fine package) after the reflow process	92
Figure 4.16:	The fillet formation of the wetted solder at different types of nanoparticles with different weight percentages (20 μ m scale).	92
Figure 4.17:	Schematic diagram of the fillet height measurement.	94

Figure 4.18:	(a) Fillet observation from the study (b) Fillet formation at the leg of chip component and PCB pad (Baated et al., 2010)	95
Figure 4.19:	Wetting angle formation at different Cu composition (Yu et al., 2004)	96
Figure 4.20:	Specified points near the base metal and the terminal of 01005 capacitor (ultra-fine package).	97
Figure 4.21:	Graph of velocity distribution of different types of nano-reinforced solder with different weighted percentages nanoparticles	99
Figure 4.22:	Graph of pressure distribution of different types of nano-reinforced solder with different weighted percentages nanoparticles.	101

LIST OF ABBREVIATIONS

2-D	2-Dimensional
-----	---------------

3-D	3-Dimensional
Ag	Silver
Ag ₃ Sn	Silver Compound-Tin
Al	Aluminum
Al ₂ O ₃	Aluminum Oxide
BaTiO ₃	Barium Titanate
BGA	Ball Grid Array
Bi	Bismuth
Ce	Cerium
CFD	Computational Fluid Dynamic
Co	Cobalt
CoSn ₂	Cobalt Compound-Tin (IMC)
CTE	Coefficient of Thermal Expansion
Cu	Copper
Cu ₃ Sn	Copper Compound-Tin (IMC)
Cu ₆ Sn ₅	Copper Compound-Tin (IMC)
(Cu,Ni) ₆ Sn ₅	Copper-Nickle-Tin (IMC)
DOE	Design of Experiment
DPM	Disperse Phase Method
EDS	Energy Dispersive X-ray Spectroscopy
EIA	Environmental Impact Assessment
EPA	Environmental Protection Agency
EU	European Union
Fe	Iron
Fe ₂ NiO ₄	Iron Nickel Oxide

Fe ₂ O ₃	Iron (III) oxide
FEM	Finite Element Method
FIB	Finely Focused Ion Beam
FSI	Fluid Structure Interface
FVM	Finite Volume Method
FVM-DPM	Finite Volume Method- Disperse Phase Method
HRTEM	High Resolution Transmission Electron Microscope
IC	Integrated Circuit
IMC	Intermetallic Compound
In	Indium
IPC-A-610	Acceptability of Electronic Assemblies
J-STD-001E- 2010	Industrial Standard, Requirements for Soldered Electrical and Electronic Assemblies
LBM	Lattice Boltzmann method
MLCC	Multi-Layer Ceramic Capacitor
NEMI	National Electronic Manufacturing Initiative
Ni	Nickle
NiO	Nickle Oxide
O	Oxygen
OSP	Organic Solderable Preservative
Pb	Lead
PCB	Printed Circuit Board
RoHS	Restriction of Hazardous Substances Directive
SAC 405	95.5Sn-3.0Ag-0.5Cu
SAC305	95.5Sn-4.0Ag-0.5Cu

Sb	Antimony
SIMPLE	Semi-Implicit Method
SMC	Surface Mount Component
SMD	Surface Mount Device
SMT	Surface Mount Technology
Sn	Tin
SEM	Scanning Electron Microscope
Sn-Ag-Cu	Tin-Silver-Copper
Sn-Cu	Tin-Copper
Sn-Pb	Tin-Lead
THT	Through Hole Technology
Ti	Titanium
TiO ₂	Titanium Dioxide
VOF	Volume of Fluid
Zn	Zinc
ZrO ₂	Zirconium dioxide

LIST OF SYMBOLS

ρ	Density of the fluid
t	Time
u	Fluid velocity in x-direction
v	Fluid velocity in y-direction
w	Fluid velocity in z-direction
C_p	Heat Capacitance
T	Temperature
K	Constant
Φ	Polar coordinate
∇	Change of derivative
$\bar{\tau}$	Shear stress
G	Gravity
Σ	Surface tension coefficients
θ	Contact angle
γ_{LG}	Surface tension of the liquid-gas
γ_{SL}	The interfacial tension liquid-solid
γ_{SG}	Surface free energy of the solid
\dot{m}	Mass transfer
S	Source term
A	Primary-phase volume fraction
f	Fluid volume fraction
F_D	Drag force
u_p	Particle velocity
ρ_p	Particle density
d_p	Particle diameter

μ	Kinematic viscosity
F_x	Additional force
D_T	Thermophoric coefficient
F_B	Brownian force
ξ	Zero-mean
S_o	Gaussian random numbers
k_B	Boltzmann constant
C_c	Cunningham factor
Λ	Particle's mean free path
N	Particle number density
F_L	Saffman's lift force
C_D	Drag coefficient
Re	Reynold number
K	Constant, 2.594
d_{ij}, d_{ik}, d_{ki}	Deformation tensor
Ψ	Particle sphericity
V_p	Volume
S_p	Surface area of particle
ϕ	the shape factor
P	Pressure
R	Real path
h	Height
Sp	Pad width
Wp	Stencil width
D	Stencil thickness

V_f	Volume fraction
H_s	Circle segment

**KAJIAN KAEDAH SEBARAN FASA PARTIKEL BAGI PENDOPAN
ZARAH-NANO DALAM PATERI SAC305**

ABSTRAK

Pada masa kini, kebanyakan peranti elektronik terdiri daripada komponen-komponen ultra-halus, oleh itu, untuk memastikan ketahanan yang tinggi dan kekuatan pada pemasangan ultra-halus dan komponen-komponen ini boleh mewakili cabaran besar untuk pereka produk. Banyak penyelidikan tertumpu kepada penggunaan pateri tanpa plumbum Sn-3.0Ag-0.5Cu (SAC305) dengan pendopan zarah-nano telah diperkenalkan kepada proses pateri ke arah peningkatan penggunaan pateri tanpa plumbum tetapi kajian terhadap kepada dapatan eksperimen. Dengan pendopan zarah-nano dalam pateri tanpa plumbum, trajektori zarah-nano sepanjang paterian proses perlu dipantau kerana ini akan mempengaruhi pembentukan ketinggian fillet, lapisan sebatian antara logam (IMC) dan pembentukan mikro-ruang kekosongan. Interaksi dua hala yang menggunakan gabungan kaedah isipadu cecair (VOF) dan kaedah fasa partikel (DPM) telah diperkenalkan dalam kajian semasa untuk menyelidik interaksi antara zarah-halus and pateri lebur. Jenis zarah-halus yang telah didopkan dalam pateri tanpa plumbum SAC305 adalah Titanium Oksida (TiO_2), Nikel Oksida (NiO), Besi (III) oksida (Fe_2O_3) partikel dengan anggaran diameter $\approx 20\text{nm}$ dan pada peratus berat zarah yang berbeza iaitu 0.01, 0.05 and 0.15 wt.% pada jenis kapasitor 01005 dengan sendi ultra-halus. Kedua jenis kajian eksperimen dan simulasi dilaksanakan untuk membandingkan kesesuaian model baru simulasi DPM. Keputusan yang diperoleh dari eksperimen dapat memvisualisasikan trajektori nanopartikel dengan berkesan pada akhir proses paterian. Simulasi DPM juga mampu menunjukkan trajektori nanopartikel secara terperinci dalam keadaan paterian haba SAC305. Di samping itu, keserasian diantara kedua-dua eksperiment dan simulasi data dapat diperoleh dalam kajian ini. Ketinggian fillet dari composite pateri juga memenuhi syarat

minima untuk kapasitor jenis 01005 seperti yang ditetapkan oleh piawaian Industri Elektronik (IPC). Keputusan kajian juga menunjukkan bahawa 0.05wt% NiO nanopartikel mempunyai masa terendah bagi membentuk fillet iaitu 2.65 saat, dan 0.05wt% Fe₂O₃ nanopartikel mempunyai trajektori sebaran zarah yang diagihkan dengan baik. Ini mempengaruhi perencatan pembantukan mikro-ruang dan membentuk lapisan IMC yang nipis. Pendopan nanopartikel dalam SAC305 mengurangkan kebolehan pembentukan IMC yang lebih selari dengan keperluan pembentukan lapisan IMC. Seterusnya, ini menyumbang kepada kebolehbaitan pembetukan pateri yang mana menghalang mikro-ruang terbentuk disebabkan pengedaran tekanan tekanan yang tinggi memberi pengaliran cairan pembentukan pateri yang baik. Kajian interaksi dua hala model VOF dan DPM menunjukkan daya maju dengan pendekatan simulasi dalam proses pematerian component kecil dengan dopan nanopartikel dan cara alternatif ini boleh memberikan kebaikan kepada pendekatan konvensional eksperimen yang mahal.

Katakunci:

SAC305; Nano-komposit pes pateri; Nanopartikel; Titanium oksida (TiO₂); Nikel oksida (NiO); Besi (III) oksida (Fe₂O₃); Simulasi berangka; Kaedah kuantiti terhad (VOF); Kaedah fasa partikel (DPM).

**DISPERSE PHASE METHOD PARTICLE STUDY WITH DOPED NANO-
PARTICLES IN SAC305 SOLDER**

ABSTRACT

Nowadays, most electronic devices consist of miniature components, therefore, to ensure high durability and strength on the assembly of these miniature joints and components can represent huge challenges to the product designer. Vast amount of researches have been concerted to the usage of nano-reinforced Sn-3.0Ag-0.5Cu (SAC305) lead free solder that is introduced to the solder paste for the improvement of the current lead free alloy but the study is limited to experimental findings only. With the inclusion of nanoparticles in the lead free solder, the trajectory of the nanoparticles throughout the soldering process needs to be monitored since it will influence the formation of the fillet height, inter-metallic compound (IMC) layer and micro-void formation. A two way interactions utilizing both volume of fluid method (VOF) and disperse phase method (DPM) are introduced in the current study to account for the interaction between both the nanoparticles and the molten solder. The nano-reinforced particles that are introduced in the SAC305 solder are titanium oxide (TiO_2), nickle oxide (NiO) and Iron (III) oxide (Fe_2O_3) nanoparticles with an approximate diameter of $\approx 20\text{nm}$ at different weight percentages of 0.01, 0.05 and 0.15 wt.% for application to ultra-fine 01005 type capacitor. Both experimental and simulation studies were conducted to compare the validity of the new DPM based simulation. The results obtained from the experiment can effectively visualize the distribution of the nanoparticles at the end of the reflow process. The DPM simulation on the other hand is capable of showing detail trajectory of the nanoparticles as it undergoes SAC305 thermal reflow. Additionally, good agreement can be seen between both experimental and simulation data obtained for all cases of nanoparticles being used. The fillet height of the nano-reinforced solder also

managed to meet the minimum requirement for 01005 capacitor as set by the Association Connecting Electronics Industries (IPC) standards. The findings also show that 0.05wt% of NiO nanoparticles has the lowest wetting time with 2.65s. Additionally, for 0.05wt% of Fe₂O₃, the trajectory of nanoparticles are well distributed leading to inhibition of void formation and thin IMC layer. The introduction of the nanoparticles in the SAC305 have also shown further retardation on the growth of IMC layer that is favorable since it is aligned with the main requirement of having a thin layer of IMC. Subsequently, this can contribute to good wettability of the solder and managed to inhibit micro-voids formation due to the higher pressure distribution that can promote the flow front propagation of the wetted solder. The study of two-ways interaction of both VOF and DPM models showed the viability of the simulation approach in simulating the miniature soldering process of the molten solder with nanoparticles and can provide a useful alternative to the conventional costly experimental approach.

Keywords:

SAC305; Nanocomposite solder paste; Nanoparticles; Titanium oxide (TiO₂); Nickel oxide (NiO); Iron (III) oxide (Fe₂O₃); Numerical simulation; Finite volume method (FVM) ; Disperse phase method (DPM).

CHAPTER ONE

INTRODUCTION

1.1 Introduction

Electronic packaging is a major discipline within the field of electronic engineering and includes a wide variety of technologies. Nowadays, there are a lot of electronic products available in the market. As time passes, we can observe the revolution of electronics in our modern days. In the ever-changing technology landscape, the industry has responded and will continue to respond to competitive demand in the global marketplace. It can be observed that the advancement of the technology have pushed the human capability beyond imagination in which we can use multi-function smartphones, get aid from robots to replace labour force and enjoy the use of sophisticated yet easy to use household electrical appliances. The requirement placed for high reliability electronic components, miniaturization of the active and passive components are forcing engineers and designers to further optimize the existing manufacturing method (Shah et al., 2006). The electronic components manufacturers have strived to meet the consumer's demand that include highly reliable and low cost components (Alam et al., 2009). The use of smaller passive components in products is expected to reduce the size of the devices manufacture though it would test the mettle of the designers to maintain or even enhance the reliability of the device (Lee, 2002). Assembling these miniature resistors and capacitors presents significant design and assembly challenges.

The advancement in the use of composite lead free solder are essential to cope with the miniaturization of the electronic components. Proper composition of soldering process, material selection, reinforced material selection and the design of

the electronic packaging becomes crucial to maintain the reliability and functionality of the electronic device. The expansion of the electronic components development is moving forward in achieving high reliability of miniaturization and diversification for various electronic packaging applications.

1.2 Surface mount devices and technologies

Most of the major electronics appliances must consist a printed circuit board (PCB) to regulate the functionality of the device. PCBs are boards that mechanically supports and electrically connects electronic components with conductive tracks, pads and other features etched from the copper sheets that is laminated onto non-conductive substrate. One of the primary insulating substrate PCB widely used is the FR-4 glass epoxy PCB.

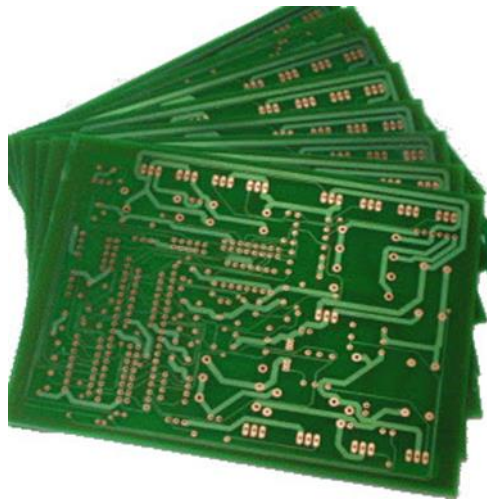


Figure 1. 1: Printed Circuit Board (PCB).

PCB assembly is a necessary step of its manufacturing process, in which either the surface mount technology (SMT) or through-hole technology (THT) is to